Interstitial cluster in FCC metals

J. Phys. F: Metal Phys., 11(1981)1161–73. Printed in Great Britain

Interstitial cluster in FCC metals

K W Ingle†, R C Perrin‡ and H R Schober
Institut für Festkörperforschung der Kernforschungsanlage, 5170 Jülich, Germany

Received 8 December 1980, in final form 12 January 1981

Abstract. Interstitial clusters in FCC metals have been studied using computer simulation techniques and three different interatomic potentials. The potentials were fitted to both ideal and defect crystal data. Clusters containing more than 10–13 interstitials were found to take the form of two-dimensional platelets whereas the smaller clusters had a three-dimensional nature. The most stable 2D and 3D configurations were always those which preserved the closest packing.

1. Introduction

The development of a detailed description of the behaviour of metals under irradiation has been hindered by the lack of an accurate knowledge of the properties of individual point defects and the manner in which they cluster. Recently, however, a number of low-temperature electron irradiation experiments have added considerably to our understanding and the following picture has emerged. Electron irradiation of metals at low temperature produces isolated interstitial atoms and vacant lattice sites (Frenkel pairs). On annealing at the lowest temperatures the close pairs of interstitials and vacancies recombine and the process has been identified with stages I_A to I_C of the resistivity recovery curves. At slightly higher temperatures the remaining single interstitials become mobile and may be annihilated at vacant lattice sites, be trapped at impurities or cluster together to form multiple interstitials (stages I_D and I_E). At higher temperatures these multiple interstitials become mobile and combine together to form larger clusters (stage II), leading eventually to the formation of interstitial dislocation loops. Qualitatively this behaviour is true for most FCC metals, although significant quantitative differences exist from metal to metal (Schilling 1978, Young 1978).

The ⟨100⟩ dumbbell configuration has been found to be the stable configuration for the single interstitial in Al, Cu and Ni (Ehrhart *et al* 1974, Haubold and Martinsen 1978, Knöll *et al* 1974). In Al di-interstitials have been observed and their atomic configuration has been identified as consisting of two parallel ⟨100⟩ dumbbells (Haubold 1975). In Cu on the other hand no di-interstitial has been found and it is thought that this defect becomes mobile at approximately the same time as or earlier than

† Present address: Generation Development and Construction Division, CEGB, Barnwood, Gloucester, England, UK.
‡ Permanent address: Theoretical Physics Division, UKAEA, Harwell, Didcot, Oxon, England, UK.

0305-4608/81/061161 + 13$01.50

MP(F) 11/6—A

the single interstitial. The corresponding activation energies are for Al $E_m^I = 0.115\,\text{eV} < E_m^{II} = 0.135\,\text{eV}$ and for Cu: $E_m^I = 0.117\,\text{eV} \geqslant E_m^{II}$. Thus the single interstitials are highly mobile in both metals, and this is also the case for Ni, Pt and Pb (Young 1978) and what might be thought of as a qualitative difference between Al and Cu can in fact be explained by rather small differences in the activation energies. With increasing cluster size the experimental determination of defect structure becomes increasingly difficult due to the simultaneous presence of different clusters. Thus using diffuse x-ray scattering techniques, only the average cluster size and an average dipole tensor can be determined (Ehrhart and Schlagheck 1974, Roberto *et al* 1978).

Anelastic relaxation experiments show that various clusters are formed which can reorient at some temperature, and are annealed at some other temperature (Robrock *et al* 1977). To date however such methods have not been successful in assigning cluster configurations to the various relaxation peaks for defects containing more than three interstitials. When the clusters become large enough to be seen in the electron microscope the experimental situation again becomes simpler since by this time they take the form of dislocation loops on {111} planes.

The aim of the present paper is to investigate the experimentally inaccessible region by means of computer simulation and extend previous work on single interstitials and the smaller clusters (Schober 1977, Dederichs *et al* 1978, Schober and Zeller 1978) which was successful in providing an interpretation of the experimental results for the first stages of clustering, i.e. up to tri-interstitials. In common with all such work the present simulations are limited by the assumptions inherent in the interatomic interaction potentials. Although the potentials used were fitted to a range of data for Cu, one cannot hope to be able to predict properties which are peculiar to Cu but rather to try and get a picture of the trends more generally common to FCC metals which will be dominated by geometrical effects and by the core repulsion. In order to get an estimate of the uncertainties involved, three different potentials were used: the Morse potential of Cotterill and Doyama (1967), a modified Morse potential also fitted to defect data and a spline potential. In the spline potential the stacking fault energy was used as an additional fit parameter.

The details of the potentials and of the computation are presented in the next section and the limitations of the method are also briefly discussed. The results for the structure, energies and dipole tensors of the stable clusters are then given in §3 and the transition from three-dimensional agglomerates to two-dimensional platelets is discussed. In the final section the results are summarised and comparisons are made with the available experimental data.

2. Computational model

The calculations reported in this paper were carried out using a real-space computer simulation technique in which the equilibrium structures and energies of lattice defects were obtained by minimising the total potential energy of a model crystallite with respect to the positions of its constituent atoms. In the present work crystallites containing up to 3500 movable atoms were used in conjunction with a modified version of the lattice handling program DEVIL developed at AERE Harwell. The energy minimisation was carried out by means of the method of conjugate gradients (Fletcher and Reeves 1964). In order to accelerate the latter and avoid spurious

metastable results the minimisation was periodically restarted during the simulations using a steepest descent technique.

Boundary conditions were supplied to the models by surrounding the region containing the movable atoms (region I) by a mantle of atoms (region II) which were held fixed in their perfect lattice positions. Since this type of boundary condition may affect the defect structures, a series of tests was carried out to examine the changes in the detailed patterns of atomic relaxations which were produced as the number of atoms in region I was varied. Models containing 19 {001} planes of atoms in each [001] direction were found to be quite acceptable in all cases. Thus larger models did not produce any significant changes in either the defect structure or the relative stabilities of the different configurations for a particular cluster size. However, in order to obtain reliable values for the energies of the larger interstitial clusters a correction term is needed to account for the energy which is effectively added to the models by holding the atoms of region II in their perfect lattice positions; in an infinite crystal all the atoms would suffer displacements. The correction term, E_{corr} is given by

$$E_{corr} \simeq \tfrac{1}{2} \sum_{n \in \text{region II}} \boldsymbol{S}(\boldsymbol{R}^n)\boldsymbol{F}(\boldsymbol{R}^n) \simeq \tfrac{1}{2} S_R \sum_{\substack{\text{boundary} \\ \text{layer}}} F_R$$

where $\boldsymbol{S}$ denotes the displacements from the perfect lattice positions $\boldsymbol{R}^n$ which would occur if the model were of infinite extent and $\boldsymbol{F}$ is the force exerted by the atoms of region I in the fixed boundary model on those of region II. S_R is the average radial displacement of the boundary layer and F_R the corresponding radial force component. For an isotropic continuum,

$$S_R \sim \text{tr } P_{\alpha\beta}/R_b^2$$

and

$$\sum_{\substack{\text{boundary} \\ \text{layer}}} F_R \sim \text{tr } P_{\alpha\beta}/R_b$$

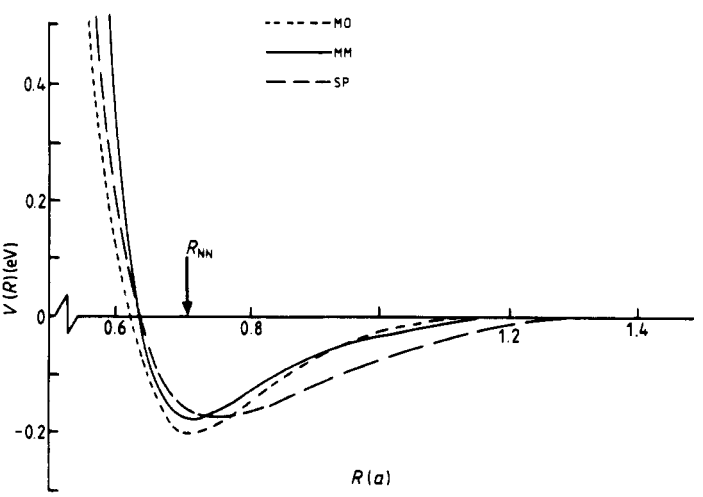

Figure 1. Morse (MO), modified Morse (MM) and spline (SP) equilibrium pair potentials for copper (a is the lattice constant, R_{NN} the nearest-neighbour distance).

where $P_{\alpha\beta}$ is the defect dipole tensor and R_b is the average radius of the boundary which is inversely proportional to the number of atoms N_I in region I. The expression for E_{corr} using this approximation thus becomes

$$E_{corr} \simeq A_c(\mathrm{tr}\, P_{\alpha\beta})^2/N_I.$$

The constant A_c may be determined by varying N_I for a particular defect and examining the resultant energy changes. A similar correction term has also been used by the Brookhaven group (R D Hatcher 1978, private communication).

Three different potentials representing copper were used in the present study, a Morse potential (MO), a modified Morse potential (MM) and a spline potential (SP). The two Morse potentials have been described elsewhere (Schober 1977, Schober and Zeller 1978) and are given by

$$V(R) = D\{\exp[-2\alpha(R - R_0)] - 2\exp[-\alpha(R - R_0)]\} + A(R - R_{NN})^4\theta(R_{NN} - R) + V_0.$$

$V(R)$ is in units of eV for

$$D = 0.18 \text{ eV (MO)}, 0.277 \text{ eV (MM)}$$

$$\alpha = 8.38526a^{-1} \text{ (MO)}, 7.6499a^{-1} \text{ (MM)}$$

$$R_0 = 0.71346a \text{ (MO)}, 0.71555a \text{ (MM)}$$

$$A = 0 \text{ (MO)}, -1200 \text{ eV } a^{-4} \text{ (MM)}$$

$$V_0 = 0 \text{ (MO)}, 0.0233 \text{ eV (MM)}$$

$$R_{NN} = a/2^{1/2}$$

and all radii are in units of the lattice parameter a. Both potentials are fitted to the vacancy formation energy, the compression modulus and the lattice parameter for copper. In addition, the modified Morse potential is matched to the relaxation volume of the single interstitial in this metal. The spline potential consisted of a set of 11 cubic polynomial segments knotted smoothly together of the form

$$V_{SP}(R) = V_i(R) \qquad \text{for } R_i \leqslant R \leqslant R_{i+1}$$

with

$$V_i(R) = \sum_{j=0}^{3} A_{ij}(R - R_i)^j.$$

The R_i are the interatomic separations at which the adjacent segments are joined, and the A_{ij} are the spline coefficients listed in table 1. The coefficients were derived in a way analogous to those for the Englert *et al* (1970) potential. In the present work great care was taken in its construction to ensure that the potential was as smooth as possible and had continuous first and second derivatives without the large kinks which are often present in spline potentials.

The experimental data used in the construction of the spline potential included the phonon dispersion behaviour (Svensson *et al* 1967), the vacancy formation energy (Bourassa and Lengeler 1976), the interstitial relaxation volume (Haubold 1975), the intrinsic stacking fault energy (Cockayne and Vitek 1974, Stobbs and Sworn 1971), the elastic constants C_{11} and C_{44} and the lattice parameter. In addition, the potential was required to reproduce the experimentally observed (Ehrhart 1978) $\langle 100 \rangle$ split or dumbbell configuration as the stable single interstitial. The most important properties of the

Table 1. The coefficients and knot positions for the spline potential. The knot positions are in Å and the coefficients have the appropriate units so that the potential is in eV. The range of the potential is 4.8708 Å.

Knot number	R_i	A_{i0}	A_{i1}	A_{i2}	A_{i3}
1	1.4500	14.203487	−71.017426	177.543594	−301.109619
2	1.5500	8.576070	−44.542007	87.210648	−61.229218
3	2.0000	0.612809	−3.249177	4.551199	−2.184472
4	2.5512	−0.161212	−0.223004	0.938955	−0.982125
5	2.8000	−0.173698	0.061835	0.205897	−0.173186
6	3.3100	−0.111582	0.136713	−0.059077	0.041636
7	3.6080	−0.074986	0.112595	−0.021855	−0.024326
8	4.1600	−0.023584	0.066231	−0.062138	−1.578438
9	4.1662	−0.023177	0.065278	−0.091497	0.116586
10	4.4189	−0.010642	0.041370	−0.003114	−0.086732
11	4.7500	−0.000434	0.010783	−0.089265	0.246316

potential are summarised in table 2, and figure 2 shows the predicted phonon dispersion curves and their fit to the experimental data. In order to fit the stacking fault energy, the potential was made relatively long-ranged, being set to zero between third and fourth nearest-neighbour distances. With such a long-ranged potential there is no need for a positive segment of $V(R)$ at $R = 2a/3^{1/2}$, and a corresponding sharp cut off, as is present in the potentials which terminate earlier (see, e.g. Englert *et al* 1970, Miller and Bristowe 1978, Miller 1980). A potential similar in shape to ours was derived by Baskes and Melius (1979).

All three potentials are of the equilibrium type and thus hold the model in equilibrium at the correct lattice parameter ($a = 3.61$ Å) without forces which depend upon the total crystal volume, i.e. the average conduction electron density. The predicted

Table 2. The properties of the spline potential.

Vacancy:	formation energy	$E_f^v = 1.268$ eV*
	relaxation energy	$\Delta V_v = -0.063$ atomic volumes
	migration energy	$E_m^v = 0.556$ eV

Single interstitials:

Interstitial type	Formation energy E_f^i (eV)	Relaxation volume ΔV_i (atomic vols)
⟨100⟩ split	2.757	1.658*
⟨110⟩ split	2.910	1.744
⟨111⟩ split	3.067	1.661
Octahedral	2.949	1.767
Tetrahedral	3.127	1.713
Crowdion	2.908	1.734

⟨100⟩ split migration energy $E_m^i = 0.060$ eV
Stacking fault: $\gamma_I = 44$ mJ m^{-2}*

Note. The specific defect properties which were matched in the construction of the potential are indicated by an asterisk (*).

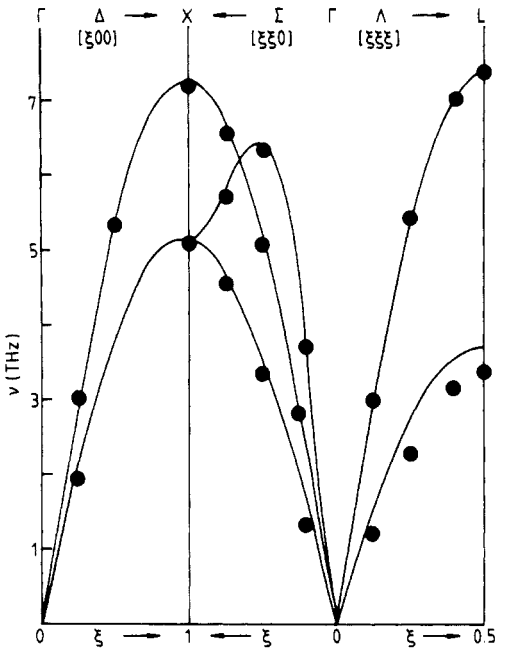

Figure 2. Comparison of the phonon dispersion of copper predicted by the SP potential with the experimental values of Svensson *et al* (1967).

elastic constants therefore satisfy the Cauchy condition, $C_{12} = C_{44}$, which is violated in real metals. It was felt better to accept this condition than to make additional assumptions about the nature of the volume-dependent term or to allow many-body interactions. Since in the present work the aim is to compare the relative stabilities of interstitial clusters containing the same number of defects, and hence having similar relaxation volumes, the effects of this assumption will be further reduced. In estimating the effects of volume forces it is important to recognise that whereas the 'Cauchy pressure' $((C_{12} - C_{44})/2)$ is made up of the contributions of first and second derivatives of the crystal energy with respect to its volume, only the first derivative contributes to the defect formation energies (Popović *et al* 1974, Finnis and Sachdev 1976, Ho 1971). To assume a constant pressure term, as is often done, is certainly too crude an approximation.

The relaxation volumes ΔV for particular point-defect configurations were calculated directly from a knowledge of the dipole tensors via

$$\Delta V = \frac{\operatorname{tr} P_{\alpha\beta}}{3\kappa}$$

where κ is the bulk modulus of the material. Two methods were used to obtain $P_{\alpha\beta}$ (Schober and Ingle 1980)

$$P_{\alpha\beta} = \sum_{n \in \text{region I}} K_\alpha^n R_\beta^n \qquad \text{or} \qquad P_{\alpha\beta} = \sum_{n \in \text{region II}} F_\alpha^n R_\beta^n$$

where $\boldsymbol{R}^n$ is the perfect lattice position of the atom n. The first method uses the first moment of the Kanzaki forces $\boldsymbol{K}^n$ defined by

$$K_\alpha^n = \sum_{m\beta} \Phi_{\alpha\beta}^{nm} S_\beta^m.$$

Here $\Phi_{\alpha\beta}^{mn}$ is the harmonic coupling constant matrix for the perfect crystal and S_β^m is the displacement of atom m. The alternative method uses the information contained in the forces which act between the atoms of region I and region II. Thus the atoms of region II are effectively subject to external forces F which restrain them from moving under the influence of the equal and opposite forces exerted by region I due to the defect. In practice the values obtained for $P_{\alpha\beta}$ by the two methods agreed to within 1% for the smaller clusters but differed by up to 10% for the largest clusters which were studied. The latter simply serves to indicate the extent of the anharmonicity in the host interatomic response. Since the boundary forces method was found to converge somewhat more rapidly than the Kanzaki forces method, the results quoted all refer to this scheme.

3. Results

One of the greatest difficulties in a computer simulation study of the structure of interstitial clusters lies in identifying the stable from the large number of metastable defect configurations. Thus for the case of the single interstitial there are six high-symmetry configurations which must be considered in addition to a number of low-symmetry structures which may also be important. The number of metastable configurations increases rapidly with increasing cluster size. Fortunately, experience in the present work soon showed that close packing is an important criterion for stability and this greatly reduces the number of geometric possibilities which needed to be studied. Furthermore the configurations with the lowest energies tended to be those in which the interstitials within a cluster acted cooperatively in displacing their host lattice neighbours. Many of the clusters which were thought to be possible candidates were found to decay to lower energy configurations. In all cases, great care had to be taken in order to ensure that the true minimum energy structures were being obtained.

The results for the most stable configurations are summarised in table 3 where values of the defect formation energies, E_f, binding energies per interstitial E_b/N, relaxation volumes $\Delta V/V_c$ and dipole tensors are given. In the region where the transition between three-dimensional (3D) clusters and two-dimensional (2D) loops occurs, values for the lowest energy configurations of both types are reported.

3.1. Structural properties of 3D clusters

The stable single interstitial configuration for all three potentials is the ⟨100⟩ split or dumbbell, figure 3(*a*). Experimentally, this is now well established as the equilibrium configuration for self-interstitials in Cu and Al (Schilling 1978). The relaxation volumes calculated for the three potentials were 2.4, 1.5 and 1.7 atomic volumes respectively; the values for the SP and MM potentials were used as parameters in their construction. The dipole tensor for this defect is weakly tetragonal.

The stable di-interstitial consisted of a pair of dumbbells centred on nearest-neighbour sites. As indicated in figure 3(*b*) these dumbbells were tilted slightly in the {110} plane. In all cases the degree of tilting was small ($<10°$) and the differences in energy between tilted and untilted configurations were less than 0.01 eV. The configuration has (110) orthorhombic symmetry.

Like the di-interstitial the stable tri-interstitial can be envisaged as consisting of a set of dumbbells on nearest-neighbour sites, figure 3(*c*). In this case however the

Table 3. Results for some important configurations.

Number of interstitials N	Type	Figure	Potential	E_f [eV]	E_b/N [eV]	$\Delta V/V_c$	tr P [eV]	p_{xx}	p_{yy}	p_{zz}	p_{yz}	p_{xz}	p_{xy}
1		3(*a*)	MO	3.8		2.4	67	1.02	1.02	0.96	0	0	0
			MM	3.4		1.5	44	1.02	1.02	0.96	0	0	0
			SP	2.8		1.7	39	1.00	1.00	1.00	0	0	0
2		3(*b*)	MO	6.4	0.61	4.5	124	1.01	1.01	0.98	0.11	0.11	−0.2
			MM	6.1	0.40	2.9	87	1.01	1.01	0.98	0.17	0.17	−0.18
			SP	4.8	0.38	3.3	77	0.99	0.99	1.02	0.09	0.09	−0.22
3	3D	3(*c*)	MO	8.6	0.96	6.2	173	1.00	1.00	1.00	0.02	0.02	0.02
			MM	8.4	0.63	4.3	129	1.00	1.00	1.00	0.02	0.02	0.02
			SP	6.5	0.58	4.7	109	1.00	1.00	1.00	0.0	0.0	0.0
4	3D	3(*d*)	MO	10.3	1.25	7.8	218	1.00	1.00	1.00	0.03	0.03	0.03
			MM	10.3	0.86	5.7	180	1.00	1.00	1.00	0.06	0.06	0.06
			SP	7.9	0.78	6.1	142	1.00	1.00	1.00	0.02	0.02	0.02
5	3D		MO	12.0	1.42	9.4	262	1.03	0.97	1.0	0.08	0.01	0.0
			MM	12.1	1.0	7.0	220	1.03	0.97	1.0	0.13	0.0	0.0
			SP	9.3	0.89	7.4	172	1.03	0.97	1.01	0.08	0.0	0.0
6	3D		MO	13.5	1.56	10.9	305	1.0	0.97	1.03	0	0	0
			MM	13.6	1.17	8.3	259	1.0	0.99	1.01	0	0	0
			SP	10.6	1.00	8.5	199	1.0	0.99	1.01	0	0	0
7	3D	3(*f*)	MO	14.6	1.72	12.3	345	1.0	1.0	1.0	0	0	0
			MM	14.5	1.36	9.3	290	1.0	1.0	1.0	0	0	0
			SP	11.5	1.12	9.5	223	1.0	1.0	1.0	0	0	0
	2D	3(*g*)	MO	15.3	1.63	12.5	353	0.92	1.04	1.04	0.32	0.25	0.25
			MM	15.5	1.21	9.8	291	0.90	1.05	1.05	0.31	0.27	0.27
			SP	12.0	1.04	10.2	237	0.91	1.045	1.045	0.30	0.23	0.23
8	3D		MO	16.8	1.71	14.0	392	1.01	1.02	0.97	0.03	0.01	0.09
			MM	16.8	1.33	10.7	331	1.01	1.01	0.98	0.0	0.0	0.07
			SP	13.2	1.11	11.2	261	1.00	1.00	0.99	0.0	0.0	0.0
13	3D		MO	24.5	1.93	22.4	626	1.0	1.0	1.0	0.0	0.0	0.0
			MM	23.6	1.60	18.2	544	1.0	1.0	1.0	0.0	0.0	0.0
			SP	19.5	1.26	17.9	419	1.0	1.0	1.0	0.0	0.0	0.0
	2D		MO	24.2	1.95	21.9	618	1.0	1.0	1.0	0.37	0.37	0.37
			MM	22.9	1.65	18.3	546	1.0	1.0	1.0	0.38	0.38	0.38
			SP	18.2	1.36	17.8	416	1.0	1.0	1.0	0.38	0.38	0.38
19	2D		MO	28.9	2.29	29.5	832	1.0	1.0	1.0	0.41	0.41	0.41
			MM	30.6	1.82	26.3	749	1.0	1.0	1.0	0.41	0.41	0.41
			SP	23.7	1.51	24.9	581	1.0	1.0	1.0	0.39	0.39	0.39
37	2D		MO	44.3	2.61	53.0	1495	1.0	1.0	1.0	0.42	0.42	0.42
			MM	47.5	2.15	49.3	1360	1.0	1.0	1.0	0.43	0.43	0.43
			SP	37.7	1.74	45.8	1071	1.0	1.0	1.0	0.41	0.41	0.41

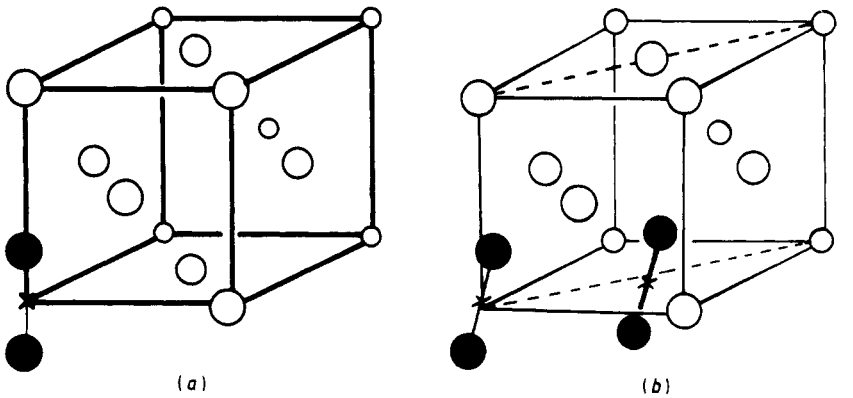

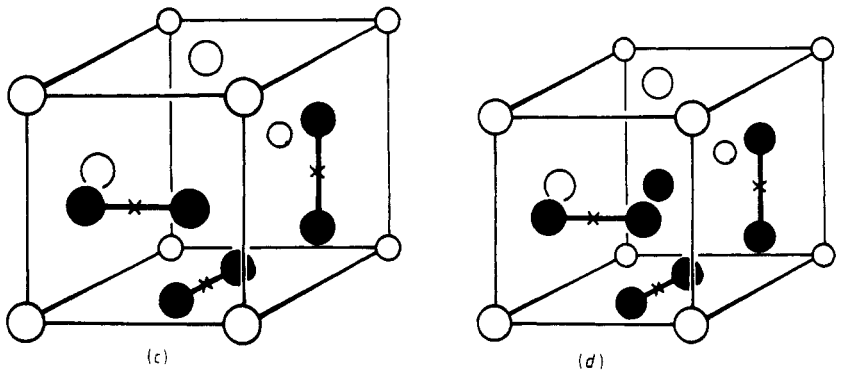

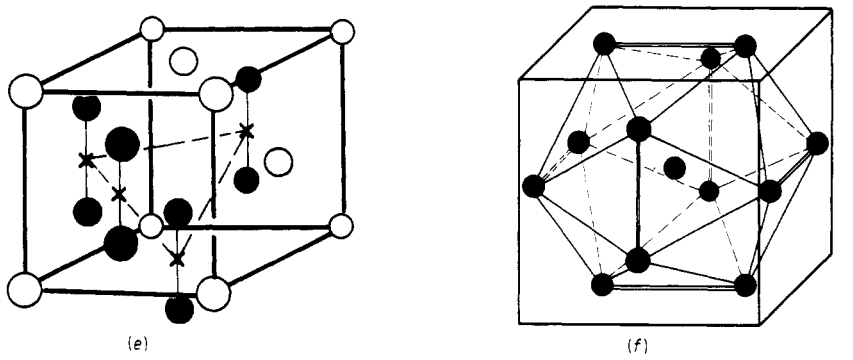

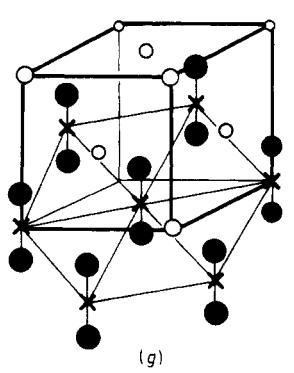

Figure 3. Schematic representation of self-interstitial cluster configurations: (*a*) single interstitial: dumbbell or ⟨001⟩ split; (*b*) di-interstitial: slightly tilted double dumbbell; (*c*) tri-interstitial: three mutually orthogonal dumbbells; (*d*) stable four interstitial cluster: 3D, three mutually orthogonal dumbbells plus an octahedral interstitial; (*e*) metastable four interstitial cluster: 2D, {111} loop split into four ⟨001⟩ dumbbells; (*f*) stable seven interstitial cluster: 3D, octahedral interstitial surrounded by six dumbbells forming an icosahedron; (*g*) metastable seven interstitial cluster: 2D, {111} platelet split in ⟨001⟩ direction.

dumbbells were arranged to be mutually orthogonal and the configuration has trigonal symmetry.

Clusters containing more than three interstitials deviated from what might have been expected by the appearance of octahedral interstitials. Thus the structure of the stable four interstitial cluster was similar to that of the tri-interstitial but involved an additional octahedral defect equidistant from each of the three dumbbells. Again this cluster has trigonal symmetry and it is shown schematically in figure 3(*d*).

The larger 3D clusters were found to be built up from the four interstitial cluster by the addition of dumbbells such that each is equidistant from the central octahedral interstitial and each lies orthogonal to its nearest-neighbour dumbbells. In this way the structure illustrated in figure 3(*f*) is built up for $N = 7$. This structure has cubic symmetry and can also be envisaged as an icosahedron centred at the octahedral site and with the surrounding dumbbell atoms as corners. It is highly stable for all three potentials considered, a fact which is reflected in the numerical results of table 3 by a fall in binding energy of the last interstitial added. The results for larger 3D clusters were based on this seven interstitial cluster with additional dumbbell or octahedral interstitials attached.

Another interesting structure was found for the case of the thirteen interstitial cluster. Surrounding the stable seven interstitial cluster by a symmetrical arrangement of six octahedrals, each a distance of one lattice parameter away from the centre of the cluster, the result of the relaxation process was that each of the constituent dumbbells moved apart into the adjacent octahedral sites. The final configuration corresponded effectively to a recrystallised region within the model. This region was shaped as an octahedron consisting of nineteen octahedral interstitials and was bounded on each face by a stacking fault. Again this structure was observed for all three potentials. A similar structure was found for vacancy aggregates by Savino and Perrin (1974).

3.2. Structural properties of 2D clusters

Whereas for large numbers of defects ($N \geqslant 13$) the 2D clusters were clearly defined as platelets of octahedral interstitials on {111} planes, the structures for the smaller defect sizes were much more complicated and indeed for the smallest sizes, 2D configurations were found to be unstable. Thus, for example, an arrangement of four octahedral interstitials on a {111} plane relaxed into a close-packed tetrahedral arrangement of dumbbells (figure 3(*c*)) and with a formation energy $E_f = 8.1$ eV (SP potential) similar to that of the stable configuration of figure 3(*d*). The equivalent result for the seven interstitial platelet was a transformation from a planar to a split planar arrangement, figure 3(*g*). In this case the two-dimensional nature of the cluster was retained and the configuration had a formation energy of 12 eV (SP). Comparing this to the value of 11.5 eV for the stable 3D configuration serves to emphasise further the stability of the latter. In general this splitting behaviour of small 2D platelets of octahedral interstitials into dumbbells was observed for all three potentials. By the time the cluster sizes approached the crossover from 3D to 2D cluster stability, the character of the 2D platelets was invariably octahedral.

3.3. Transition from 3D to 2D clusters

Figure 4 illustrates for both 2D and 3D clusters the variation of formation energy per interstitial E_f/N for the most stable configuration with cluster size N. Since all three

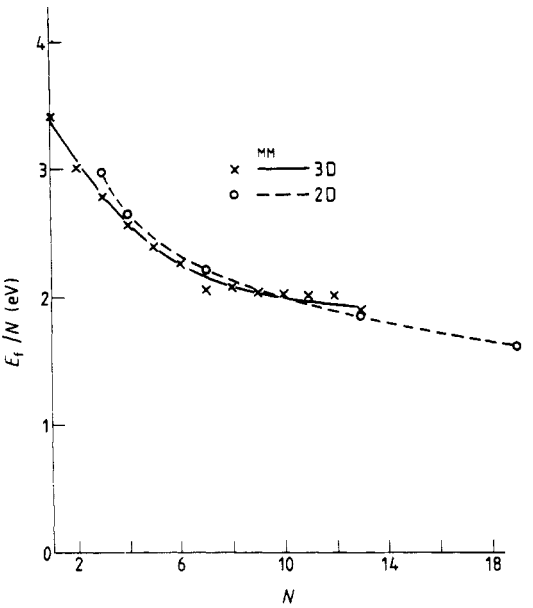

Figure 4. Variation of formation energy per interstitial (E_f/N) for the 3D and 2D cluster configurations as a function of cluster size N (MM potential). Lines are guides to the eye only.

potentials used give a similar behaviour only the values for the MM potential are shown. For all three potentials 3D clusters are more stable for $N < 9$ whereas 2D clusters are preferred for $N > 13$. In order to assess the likelihood of any particular interstitial cluster arising in practice, the details of the way in which clusters may be formed, reorient and grow must be known in addition to the basic stability data. For the latter the migration energies of the smaller clusters are particularly important. The migration mechanisms for the smallest clusters have already been reviewed for the MO and MM potentials (Schober 1977, Schober and Zeller 1978) and the same mechanisms were found to hold in the present work for the SP potential.

The single interstitial is highly mobile with predicted values for E_m^I of 0.07, 0.12 and 0.06 eV obtained for MO, MM and SP respectively. The corresponding experimental value is 0.12 eV for Cu and Al. Depending on the potential the di-interstitial is either less mobile (MO:$E_m^{II} = 0.14$ eV) or more mobile (MM:$E_m^{II} = 0.10$ eV) than the single interstitial. In nature the two different cases are realised in Al and Cu respectively. For the larger clusters the mobility decreases rapidly with increasing cluster size. Thus for the MO potential values of $E_m^{III} = 0.21$ eV, $E_m^{IV} = 0.31$ eV, $E_m^{V} = 0.35$ eV were obtained. Whereas for clusters containing up to three interstitials the migration mechanism can be thought of as consisting of single interstitial jumps the migration of a five interstitial complex involves a rather complex collective motion of the whole cluster. The existence of diffusion channels (Johnson 1966) for the migration of the single interstitial would not be expected to play a role in the formation of the larger clusters since the energy needed to change from one channel to another one was, for all three potentials, low.

Although the migration energies were found to increase with increasing cluster size this was not observed to be the case for the activation energies for reorientation processes. Thus, for example, the reorientation of the stable tri-interstitial (Robrock *et*

al 1977) occurs by means of an intermediate metastable configuration which has an E_f close to that of the stable configuration.

In the transition region, where the relative stability of 3D and 2D clusters is reversed, there are stable and metastable configurations with similar energies. It is plausible that low activation energy mechanisms link these configurations. During the formation of the larger clusters from smaller ones a binding energy of several eV is gained (e.g. $I_3 + I_5 \rightarrow I_8 + 2.5$ eV). This binding energy release can be thought of as localised mostly in the cluster and its nearest neighbours, and thermal activation in the real crystal could result in the necessary atomic rearrangements resulting in the formation of the lowest energy configuration.

4. Discussion

For all three potentials considered in this paper similar trends have been found for the relative stabilities of the interstitial clusters. Thus, for example, there is a strong increase of the binding energies with increasing cluster size, and the binding energies of the stable configurations are always much larger than the activation energies for migration. A break-up of interstitial clusters can therefore be ruled out. The small clusters preferentially adopt three-dimensional configurations with the close packing of the constituent interstitials playing an important role. Particularly stable cluster configurations are obtained when the interstitials are arranged in a highly symmetric way. In particular, a very stable, elastically isotropic, complex with cubic symmetry can be built up for seven interstitials. Larger clusters ($N \geqslant 13$) are preferentially two-dimensional and again the most closely packed configurations have the lowest energies and are therefore the most stable. The crossover between three- and two-dimensional cluster stability is in rough agreement with the experimental observations for Cu and Al (Ehrhart and Schilling 1973, Roberto *et al* 1978). Unfortunately, however, the experimental information is not detailed enough to allow a stringent test to be made on the results obtained from the present models.

For the smaller clusters ($N < 7$) the activation energy for diffusion was found to increase with increasing cluster size. One exception to this was the di-interstitial which could, depending on the potential chosen, be either more or less mobile than the single interstitial. With the possible exception of the highly symmetric types, the cluster can reorient with relative ease. It is expected that the binding energy gained in the formation of larger clusters from smaller ones is sufficient for the clusters to attain their stable configurations. More detailed work on this latter point is needed, however.

In common with all other similar calculations the present methods suffer from the uncertainties involved in the construction of interionic potentials. We cannot claim that our results will reproduce exactly the absolute values of the defect energies in copper. However, since all three potentials predict the same types of defect structures these should be typical for many FCC metals although slight changes in energies can change the relative stabilities from one metal to another.

Acknowledgment

One of the authors (KWI) wishes to acknowledge the financial support given to him during his stay at Jülich by the Alexander von Humboldt Foundation.

References

Baskes M I and Melius C F 1979 *Phys. Rev.* B **20** 3197.
Bourassa R R and Lengeler B 1976 *J. Phys. F: Met. Phys.* **6** 1405
Cockayne D J H and Vitek V 1974 *Phys. Status Solidi* b **65** 751
Cotterill R M J and Doyama M 1967 *Lattice Defects and their Interactions* ed R R Husigutti (New York: Gordon and Breach)
Dederichs P H, Lehmann C, Schober H R, Scholz A and Zeller R 1978 *J. Nucl. Mater.* **69–70** 176
Ehrhart P 1978 *J. Nucl. Mater.* **69–70** 200
Ehrhart P, Haubold H G and Schilling W 1974 *Adv. Solid State Phys.* **14** 87
Ehrhart P and Schilling W 1973 *Phys. Rev.* B **8** 2604
Ehrhart P and Schlagheck U 1974 *J. Phys. F: Met. Phys.* **4** 1589
Englert A, Tompa H and Bullough R 1970 *Fundamental Aspects of Dislocation Theory NBS Special Publication* 317 (Washington DC: US Government) p 273
Finnis M W and Sachdev M 1976 *J. Phys. F: Met. Phys.* **6** 965
Fletcher R and Reeves C M 1964 *Comput. J.* **7** 149
Haubold H G 1975 *Proc. Conf. on Fundamental Aspects of Radiation Damage in Metals* CONF-751006-P1 (USERDA)
Haubold H G and Martinsen D 1978 *J. Nucl. Mater.* **69–70** 644
Ho P S 1971 *Phys. Rev.* B **3** 4035
Jäger W and Urban K 1977 *Comment. Phys.* **2** 15
Johnson R A 1966 *Phys. Rev.* **152** 629
Knöll H, Dedek U and Schilling W 1974 *J. Phys. F: Met. Phys.* **4** 1095
Miller K M 1980 *Phys. Status Solidi* b **98** 387
Miller K M and Bristowe P D 1978 *Phys. Status Solidi* b **86** 93
Popović Z D, Carbotti J P and Piercy G R 1974 *J. Phys. F: Metal Phys.* **4** 351
Roberto J B, Schoenfeld B and Ehrhart P 1978 *Phys. Rev.* B **18** 2591
Robrock K H, Rehn L E, Spirič V and Schilling W 1977 *Phys. Rev.* B **15** 680
Savino E J and Perrin R C 1974 *J. Phys. F: Met. Phys.* **4** 1889
Schilling W 1978 *J. Nucl. Mater.* **69–70** 465
Schober H R 1977 *J. Phys. F: Met. Phys.* **7** 1127
Schober H R and Ingle K W 1980 *J. Phys. F: Met. Phys.* **10** 575
Schober H R and Zeller R 1978 *J. Nucl. Mater.* **69–70** 341
Stobbs W M and Sworn C H 1971 *Phil. Mag.* **24** 1365
Svensson E C, Brockhouse B N and Rowe J M 1967 *Phys. Rev.* **155** 619
Young F W 1978 *J. Nucl. Mater.* **69–70** 310